Scanning Microscopy

Volume 1 | Number 4 Article 13

6-8-1987

Electron Probe Micro-Analysis and Laser Microprobe Mass Analysis of Material Leached from a Limestone Cathedral

L. A. Leysen
University of Antwerp

J. K. De Waele
University of Antwerp

E. J. Roekens
University of Antwerp

R. E. Van Grieken
University of Antwerp

Follow this and additional works at: https://digitalcommons.usu.edu/microscopy

 Part of the Biology Commons

Recommended Citation

Leysen, L. A.; De Waele, J. K.; Roekens, E. J.; and Van Grieken, R. E. (1987) "Electron Probe Micro-Analysis and Laser Microprobe Mass Analysis of Material Leached from a Limestone Cathedral," *Scanning Microscopy*: Vol. 1 : No. 4 , Article 13.
Available at: https://digitalcommons.usu.edu/microscopy/vol1/iss4/13

This Article is brought to you for free and open access by the Western Dairy Center at DigitalCommons@USU. It has been accepted for inclusion in Scanning Microscopy by an authorized administrator of DigitalCommons@USU. For more information, please contact digitalcommons@usu.edu.

Scanning Microscopy, Vol. 1, No. 4, 1987 (Pages 1617-1630)
Scanning Microscopy International, Chicago (AMF O'Hare), IL 60666 USA

0891-7035/87$3.00+.00

ELECTRON PROBE MICRO-ANALYSIS AND LASER MICROPROBE MASS ANALYSIS OF MATERIAL LEACHED FROM A LIMESTONE CATHEDRAL

L.A. Leysen, J.K. De Waele, E.J. Roekens and R.E. Van Grieken*

Department of Chemistry, University of Antwerp (U.I.A.)
Universiteitsplein 1, B-2610 Wilrijk, Belgium

(Received for publication February 28, 1987, and in revised form June 08, 1987)

Abstract

Electron probe X-ray micro-analysis (EPXMA) and Laser microprobe mass analysis (LAMMA), were applied to characterize the leachate of sandy limestones of a Belgian cathedral.

Individual suspended particles, found in water that was sprayed over the cathedral walls ("leachate water"), were sized and analyzed by automated EPXMA-analysis, and classified with hierarchical cluster methods. LAMMA was used to gather more information about particles, present in the solution, as well as in suspension.

It was found that the leachate from black walls, had a high sulphate concentration and a large variety of particles in suspension, with different morphology and composition, with silicates as most abundant group. The leachate from white walls is characterized by a predominant Ca-rich suspension, with both original and recrystallized calcite particles, and by a much lower sulphate- ion concentration in the solution.

LAMMA-analysis revealed that the "organic" group of the EPXMA-analysis, consists mostly of carbon-containing fly-ash particles.

Hence, in general, it could be concluded that walls which are not subject to direct rainfall are generally covered with a gypsum crust, that turns black due to adhesion of soil dust and fly-ash particles, while white walls become thinner due to rainwater erosion of weathering products and original stone components.

KEY WORDS : Electron probe X-ray micro-analysis (EPXMA), Laser microprobe mass analysis (LAMMA), weathering study, limestone-deterioration, air pollution, leachate, historical building.

*Address for correspondence :
R. Van Grieken, Department of Chemistry, University of Antwerp - U.I.A., Universiteitsplein 1, B-2610 Wilrijk (Belgium)
Phone No. (03)828.25.28

Introduction

The accelerated deterioration of various materials induced by air-pollution has recently received much attention. Especially historical buildings and monuments are the subject of various international research projects, as appears from numerous recent publications, review articles [6], and conferences [16], concerning this topic. Although already much has been published on the air pollution induced formation of a gypsum crust on carbonate stones, additional research is warranted for the following reasons. The exact contribution of NO_x and HCl induced weathering compared with the SO_2 induced weathering has not been documented clearly. Yet, in view of the different sources of these components, such knowledge is essential for a relevant pollution abatement strategy. The role of catalytic agents in the decay process like carbonaceous and fly-ash particles, or other particles or trace elements which may have been overlooked until now, should be further elucidated. Indeed, results obtained by simulation processes in reaction chambers, in which stone specimens are exposed to high SO_2 levels, often deviate from real out-door weathering, probably due to the absence of catalysts for the sulphatation process [22]. Measurement of decay rates and establishment of damage functions are essential in order to define the qualitative and quantitative resistance of stone materials to the effects of air pollution.

About 2 years ago, our laboratory started a detailed study on the chemical weathering of the 13th-15th century St. Rombout's Cathedral in Mechelen, a town in the north of Belgium. This cathedral was selected because it is situated in the heavily industrialized area between Antwerp and Brussels, and especially because it is a representative example of material use and architecture of many large historical buildings in Flanders and the Low Lands. The cathedral was originally built of sandy limestone from Balegem and Gobertingen, Belgium. These contain about 40-60 % and 10-20 %, respectively, of rather fine quartz grains, cemented by a microcrystalline calcium carbonate matrix [15].

Since those building stones are very sensitive to air pollution-induced weathering, a detailed and thorough examination of the decay mechanism was carried out. This should give a scientific basis to guide the actions and policy with respect to building protection and restoration works, and could result in a methodology to study other affected buildings and stone materials.

Different trace and micro-analytical techniques were used to study the weathering of this building [9,11,18]. The results showed that practically every wall was covered with a weathering crust, varying greatly in thickness, colour and composition. Some striking differences were noticed as a function of the orientation of the wall towards wind and hence precipitation direction. At the East side of the building, usually not exposed to precipitation, a 300-1000 µm thick outer crust of micro-crystalline gypsum, containing carbonaceous particles was observed, which was very clearly different from the apparently unaffected part of the stone. At the West side, this surface layer was mostly eroded away due to precipitation, and the walls have a fresh and clear appearance. At the North and South side, the weathering crust is more irregular. All analyzed crust samples showed a much larger contribution of S-containing weathering products, relative to the contribution of N- and Cl-containing weathering compounds. The pH of rainwater (5.8) and of total deposition (6.7), collected near the cathedral, was slightly alkaline compared to the normal pH value (5.6) of pure rainwater. These observations led to the conclusion that attack by gaseous atmospheric compounds, especially SO_2, is highly important in the total chemical deterioration process, and that rainwater is not an offending medium but plays a role as wetting and eroding medium.

In order to study the deterioration mechanisms in more detail and to make an accurate diagnosis of the role of rainwater in the process, it is of interest to examine the composition of rainwater that has run down over the walls of the building ("run-off water"). Study of run-off water can indeed lead to : establishment of quantitative material loss and decay rates, detection of reaction products that are easily removed by the rain, identification of stone components that are preferentially eroded by the action of the rainwater, and thus constitute weak points in the stone structure [12].

As an alternative, leaching experiments were performed by isolating a certain area of the building wall and by spraying this stone with demineralized water. The leaching technique was evaluated versus the results obtained by analysis of run-off water sampled in integrating collectors [10,19] since it is not dependent on the characteristics of the rainfall events and allows to isolate and study specific wall sections . The identification of suspended particles in the deposition and run-off samples, obtained by automated electron probe X-ray micro-analysis, combined with hierarchical cluster analysis [1], showed an important difference in number, as well as in composition of the suspended particles in run-off and rainwater [10] . This paper reports the micro-analytical examination of the water samples collected during the leaching experiment.

Materials and Methods

Method

On October 6, 1986 a leaching experiment was done at the St. Rombout's Cathedral in Mechelen. Onto both a black and a white wall section, located just near to each other, a plastic frame of 28.5 x 45.5 cm was pressed, to isolate a surface area of 1300 cm^2. On each section, deionized water was sprayed three consecutive times during two minutes at a rate of 300 ml/min. Six samples were obtained : three for the white wall, hereafter called W-1, W-2 and W-3, and three for the black wall, called B-1, B-2 and B-3. Two blanks were taken by placing a PVC-plate at the back of the frame and spraying water onto this plate. The individual suspension particles in all the collected samples were thoroughly studied using electron probe X-ray micro-analysis (EPXMA) and laser microprobe mass analysis (LAMMA), in order to elucidate the difference in composition between particles found in the leaching water from white and black wall sections.

Apparatus

The EPXMA-measurements were performed with a JEOL JXA-733 Superprobe (Jeol Ltd., Tokyo, Japan), used at an electron energy of 25 keV and a beam current of 1 nA. The characteristic X-rays generated by the electron beam are measured with energy-dispersive (ED) and wavelength-dispersive (WD) X-ray spectrometers. (It is well known that elements lighter than Na, such as C, N and O, do not yield measurable X-ray signals in EPXMA, while high-Z elements also exhibit a low sensitivity). The electron microprobe is also equipped with a secondary electron and transmission electron detector, and backscattered electron detectors (for composition and topographic viewing). The magnification was 480x. The microprobe is automated with a Tracor Northern TN 2000 system and controlled by an LSI 11/23 minicomputer with two double-density floppy disk drives. The Tracor software was somewhat modified to obtain greater flexibility. In the modified PRC (Particle Recognition and Characterization) computer program, particles are localized according to their backscattered electron signal. The electron beam performs consecutive line scans over the image field. The locations of objects are marked by contour points, where the image intensity drops below or jumps above the threshold value. The coordinates of these contour points are stored in the memory. When a contour line is found to be closed, the particle is analyzed before the line scan continues. For each particle, all contour pixel coordinates are known. The area (A) of the particle is the total number of pixels enclosed by the contour line, multiplied by the area represented by one pixel. The equivalent

diameter D of a circular particle with the same area is then calculated according to the formula $D = 2\sqrt{\frac{A}{\pi}}$. The perimeter is simply the sum of the distances between the contour pixels. From the area A and the perimeter, a shape factor is calculated. An ED X-ray spectrum is taken when the electron beam is rastered over the particle area [17]. In this way, 450 particles were sized and analyzed in each sample. Afterwards, the particles were classified by hierarchical cluster analysis [14,20] according to their chemical composition expressed as the relative intensity (normalized to a sum of 100 %) of the K X-rays from Mg, Al, Si, P and S and the K_α X-rays from K, Ca, Ti and Fe. Bernard et al. [1] have found that, for environmental applications, the most advantageous procedure was the use of hierarchical cluster analysis, based on Ward's error sum strategy.

LAMMA-measurements were performed with the LAMMA-500 instrument (Leybold-Heraeus, Cologne, FRG), which is described in detail in the literature [5,7,8,23]. In this technique, the pulsed laser light (λ = 265 nm, τ = 15 ns) of a Q-switched frequency quadrupled Nd:YAG laser (maximum power density of 10^{11} W.cm^{-2} is focused onto the sample through an optical microscope with the aid of the red spot of a continuous low power pilot He-Ne laser beam, whose optical path is collinear with the path of the high power laser. The laser beam power density can be attenuated by a 25-step optical filter system. The laser generated ions are accelerated by an Einzel-type lens and analyzed in either the positive or negative ion mode in a time-of-flight mass spectrometer, which includes an ion reflector in the drift tube. The ions are detected by an open Cu-Be secondary electron multiplier and the output signal is stored in a LeCroy 32 Kbyte memory transient recorder. The transient recorder system is controlled by an IBM-PC AT, which provides the data acquisition, display and data analysis facilities [21].

Sample preparation

Immediately after sample collection, a suitable volume (2 ml for the "white" and "black" samples, and 50 ml for the "blanks") was filtered on a 0.4 µm pore-size Nuclepore membrane filter. Of this filter, a small piece was cut off and mounted on a plastic ring. The sample was then carbon coated, and fitted into a copper sample holder for EPXMA-analysis.

For the LAMMA-experiments, about 10 µl of the collected sample was spotted onto a thin Formvar foil, supported by a standard copper electron microscopic grid. The solution was evaporated by leaving the samples overnight in a laminar flow hood. The grids were then ready for introduction into the LAMMA-instrument.

Results and Discussion

Electron microprobe study

As two typical examples of the combined automated EPXMA and computerized hierarchical cluster analysis, the detailed results for samples B-1 and W-2 are presented in Tables 1 and 2 respectively. The obtained cluster groups are ordered according to the element that yielded the most intense X-ray signal. The number of particles, the percent abundance, the average diameter and the composition, as represented by the characteristic X-ray signals, are all given. The relative abundance of the most important groups and the total number of suspended particles are included in Table 3 for the black and white leaching samples and the blanks. From those results, it is evident that there exists a rather large difference in the composition of the suspended particles in leaching water from black and white wall sections. The most obvious fact is that the Si-rich group is of major importance in leachates from black wall sections, while the white walls yield a predominant Ca-rich group. Indeed the Si-rich group amounts up to 74 % on the average for the "black" samples, while it has only a contribution of 24 % in the "white" samples; the Ca-rich group however contributes 71 % in the "white" samples, where it gives only 3.1 % in the "black" samples.

The rather small Ca-rich group in the "black" samples consists of $CaCO_3$, $CaSO_4$ and $CaSO_4$-containing particles. On the other hand, the white wall sections release no pure $CaSO_4$ particles. This fact is in good agreement with results published earlier, on the composition of crust samples [11]. It is also in accordance with the bulk composition of the solution from which the suspension was taken. The solution from black wall sections contained on the average 15 ppm Cl^-, 31 ppm NO_3^- and 725 ppm SO_4^{2-}, where that from the white wall sections contained only 3.3 ppm Cl^-, 6.3 ppm NO_3^- and 101 ppm SO_4^{2-}. Hence, it seems quite logical to find some undissolved $CaSO_4$-particles in the suspension from the black wall section samples. This finding confirms the important role of rainwater as an eroding agent; the weathering products $CaSO_4.2H_2O$, $Ca(NO_3)_2$ and $CaCl_2.6H_2O$, formed by the action of atmospheric S-, N- and Cl-containing pollutants, are solubilized in the overflowing rainwater in the case of the white walls. In sections that are shielded from direct rainfall, the weathering products remain as a crust on the wall. The Cl^--enrichment of the solution is probably caused by the deposition of NaCl-aerosols on the stone. It appears that, except in one case, the concentration of Cl^-, NO_3^- and SO_4^{2-} all gradually decrease when consecutive sprays are performed. These results however, will be discussed elsewhere [19]. The Ca-rich group in the suspension from "white" samples has a more diverse composition, besides pure $CaCO_3$ particles, the major group in all three W-samples, it includes $CaCO_3$-containing particles, together with particles containing also elements like Si, Al, Fe, Cu and Zn. Also a group with varying, but important amounts of Ca, Fe, Si and Al is present; this

Table 1 : Classification by hierarchical clustering of the EPXMA-data of the suspension particles in sample B-1.

Group no.	Most abundant element	Number of particles analyzed	% abundance of the group	AVD* ± SD (µm)	Composition expressed as average percent X-ray intensity relative to the sum of the X-ray counts								
					Mg	Al	Si	P	S	K	Ca	Ti	Fe
1	Ca	11	2.4	1.1 ± 0.3	0	0	18	0	35	0	41	0	1.0
2		8	1.8	2.5 ± 3.2	3.9	0	3.9	0	0	0	79	0	0.2
3	Si	62	13.8	2.0 ± 2.0	0	17	58	0	0.7	4.0	0.1	0	20
4		57	12.7	1.9 ± 1.5	0	25	59	0	0.4	5.6	1.7	0	0.8
5		56	12.4	1.9 ± 3.3	0	0	99	0.2	0	0	0	0	0.1
6		47	10.4	1.2 ± 0.7	0	0	69	0	0.2	0	0.1	0	30
7		37	8.2	1.0 ± 0.5	0.7	0	63	0	0.2	0.9	0	0	0
8		34	7.6	1.7 ± 1.3	0.5	13	39	1.2	7.0	0.2	5.7	0	32
9		13	2.9	1.3 ± 0.5	0	0.6	57	0	4.0	0	22	0	12
10	Fe	21	4.7	1.0 ± 0.4	0	0	3.0	0	5.3	0	0	0	86
11		17	3.8	1.3 ± 0.7	0.9	0.4	34	2.3	1.1	0.3	1.4	0	57
12	Al	2	0.45	1.2 ± 0.6	0	82	11	0	0	0	0	0	7.7
13	S	8	1.8	1.0 ± 0.5	0	1.5	23	0	26	0	0	14	0
14		2	0.45	2.4 ± 0.7	0	0	0	0	100	0	0	0	0
15	Organic	75	16.7	1.1 ± 0.6	0	0	0.8	0	0	0	0	0	0

* = average diameter ± standard deviation.

Table 2 : Classification by hierarchical clustering of the EPXMA-data of the suspension particles in sample W-2.

Group no.	Most abundant element	No. of particles analyzed	% abundance of the group	AVD* ± SD (µm)	Composition expressed as average percent X-ray intensity. relative to the sum of the X-ray counts								
					Mg	Al	Si	P	S	K	Ca	Ti	Fe
1	Ca	235	52.2	4.1 ± 3.0	0	0	0.3	0	0	0	85	0	0.1
2		70	15.6	3.6 ± 2.9	0.2	2.9	3.3	0	0.1	0	78	0	0.6
3		12	2.7	3.9 ± 3.9	0.2	7.4	18	0	0.3	0.8	59	0	3.9
4		5	1.1	2.3 ± 1.3	0	9.6	24	0	2.6	2.6	38	0	18
5	Si	28	6.2	3.6 ± 2.4	0.1	12	71	0	0.1	2.5	6.4	0	3.0
6		22	4.9	2.6 ± 1.8	0.1	12	54	0	0.2	7.4	3.9	0	21
7		14	3.1	3.0 ± 2.7	0	33	53	0	0	7.9	1.7	0.2	2.0
8		12	2.7	3.5 ± 3.1	0	0	100	0	0	0	0	0	0
9		12	2.7	4.1 ± 3.6	0	12	41	0	3.7	2.4	19	0	15
10		8	1.8	2.6 ± 1.3	0	16	59	0	0	21	1.0	0	1.8
11		1	0.22	0.8 ± -	0	0	47	44	0	0	0	0	0
12	Fe	14	3.1	2.3 ± 1.5	0	13	37	0	0.5	0.9	5.2	0	38
13		10	2.2	1.5 ± 0.5	0	3.1	7.9	0	1.0	0	1.8	0	74
14	Al	6	1.3	2.1 ± 1.1	0	16	3.8	2.4	3.2	2.7	6.4	4.0	3.2
15	Ti	1	0.22	3.5 ± -	0	0	6.9	0	0	0	17	53	13

* Average diameter ± standard deviation.

consists probably of conglomerate particles like Ca-silicates, and Ca-[Fe-Al]-silicates. Although the Ca-rich group is predominant in the suspension from white walls, the solution only contains 35 ppm Ca^{2+} on the average, while the Ca^{2+} level in leaching water from the black walls amounts to 223 ppm [19]. This can be explained through the solubility of $CaSO_4.2H_2O$ and $CaCO_3$; the former, being much more soluble, gives rise to a high Ca^{2+} concentration in solution from black walls, while the washing of $CaCO_3$-particles gives rise to a predominant Ca-rich suspension in "white" samples. Also, through frequent wetting by rainwater, the stone of white walls is becoming more porous and hence more sensible towards further erosion of structural $CaCO_3$-material.

The Si-rich group varies somewhat in the suspension of both kinds of samples. The SiO_2 subgroup ranges from 20.7 % to 2.7 %. This group can originate from soil-derived quartz, that is deposited on the stone's surface, but also from

Table 3 : Relative abundance (%) of the different particle types in suspension of the run-off samples from black and white walls and blanks

Most abundant element	Sub-group	Percent abundance B-1	B-2	B-3	W-1	W-2	W-3	Blank-1	Blank-2
Ca	* Ca only ($CaCO_3$)	-	-	-	39.1	52.2	55.6	19.3	19.1
	* Ca>70%, Si or other trace elements < 30%	1.8	0.44	-	25.8	15.6	9.1	-	-
	* Ca ,S (gypsum)	2.4	-	3.1	-	-	-	-	-
	* Ca, Si, Al, Fe	-	-	-	2.9	3.8	1.6	3.3	2.7
	* others	-	-	1.6	8.7	-	-	-	-
	Total	4.2	0.44	4.7	76.5	71.6	66.2	22.7	21.8
Si	* Si only or Si >70% and other trace elements < 30 % (SiO_2)	20.7	13.3	11.1	3.6	2.7	7.3	6.0	6.9
	* Si, Al	12.7	24.9	20	6.4	9.3	10.9	21.8	24.2
	* Si, Fe	31.8	37.3	22.7	5.3	4.9	4.9	7.1	10.7
	* Si, Ca	2.9	3.6	-	2.9	2.7	3.6	-	-
	* others	-	-	20.2	4.0	2.0	-	-	-
	Total	68	79	74	22.2	21.6	26.7	34.9	41.8
Fe	Total	8.4	13.8	12.9	1.1	5.3	5.1	28.4	19.8
S	Total	2.2	0.44	3.1	-	-	0.22	0.89	2.00
Organic	Total	16.7	3.3	-	-	-	-	-	-
Miscellaneous	Total	0.44	2.9	5.3	0.22	1.6	1.8	13.1	14.7
Number of particles per ml solution		$3.2.10^6$	$3.2.10^6$	$2.1.10^6$	$1.3.10^6$	$1.1.10^6$	$0.31.10^6$	3400	12.200

leaching of quartz grains out of the stone, because these form an important structural composite [15]. The SiO_2 is probably more abundant in the leachate from the black wall sections, because these are never cleaned by natural overflowing rainwater. Al- and/or Fe-silicates also form an important part of the Si-rich group; elements like K, S and Ca and sometimes also Cu and Zn were detected in a minor contribution here. In these groups, there can exist a slight contribution of glauconite, which is leached out of the stone [15], but the major part will result from soil dust and fly-ash particles. The group denoted as "others" involves different Si-rich sub-groups, such as groups with Si-Cu, Si-K and Si-P, accompanied by various other elements.

In the leachates from the white wall section, the Ca- and Si-rich groups together, contribute about 95 % on the average to the total composition. In the "black" samples, this average amounts only up to 77 %, while the Fe-rich group, and in some cases, the organic and miscellaneous groups, are also important.

The Fe-rich group accounts for, on the average, 11.7 % and 3.8 % in "black" and "white" samples respectively. In both series, this group consists of Fe-oxides, Fe-silicates and conglomerate Fe-containing particles. These particles can result from the scaffold, which is constructed around the cathedral for the restoration works or from leaching of glauconite. Indeed they also give a larger contribution to the blanks and, to some air samples, which were analyzed in a similar way as described before, in order to gather also information about the chemical composition of the suspended particulate in the air around the cathedral.

Particles with high electron backscatter, but no characteristic X-ray lines, are considered to be organic. This organic group consists of biological material (clumps and spores), fly-ash and other carbon-rich particles, and appears only in samples B-1 and B-2, but not in the W-samples. As will be explained below, there is evidence to believe that this group consists mostly of carbonaceous particles that adhere to the weathering crust and are responsible for the black colour of most walls, which are not under the influence of direct rainfall.

The miscellaneous group contains mostly Al- and Ti-rich groups, but also Ba-, Cu-, P-, Zn-, Ni-and Cl-rich groups are present. Actually this diverse class forms a minor contribution to the total composition and, considering the fact that it is especially found in the blanks, and in samples of air, taken around the cathedral, it could be concluded that most of these particles are pollution induced.

The last group to be considered is the one that contains particles yielding mostly X-rays from S only, i.e. consisting of S and low-Z elements. This S-rich group appears especially in the "black" samples. It includes some conglomerates. Probably the characteristic oil-fired carbonaceous particles, that are considered to be important in the deterioration of marble because they have a large specific surface area and a high sulphate content, and which are responsible for the black colouring of non-wetted walls [2,3,4], contribute also to this S-rich group. Early results however [11], indicated that these particles were only scarcely found in the surface crust samples, and so they will play a minor role in the deterioration process of this cathedral.

In order to gather more information about the contribution of coal and oil fly-ash, and about the morphological features of the automatically characterized particles some manual analyses were also performed. Fig. 1 represents

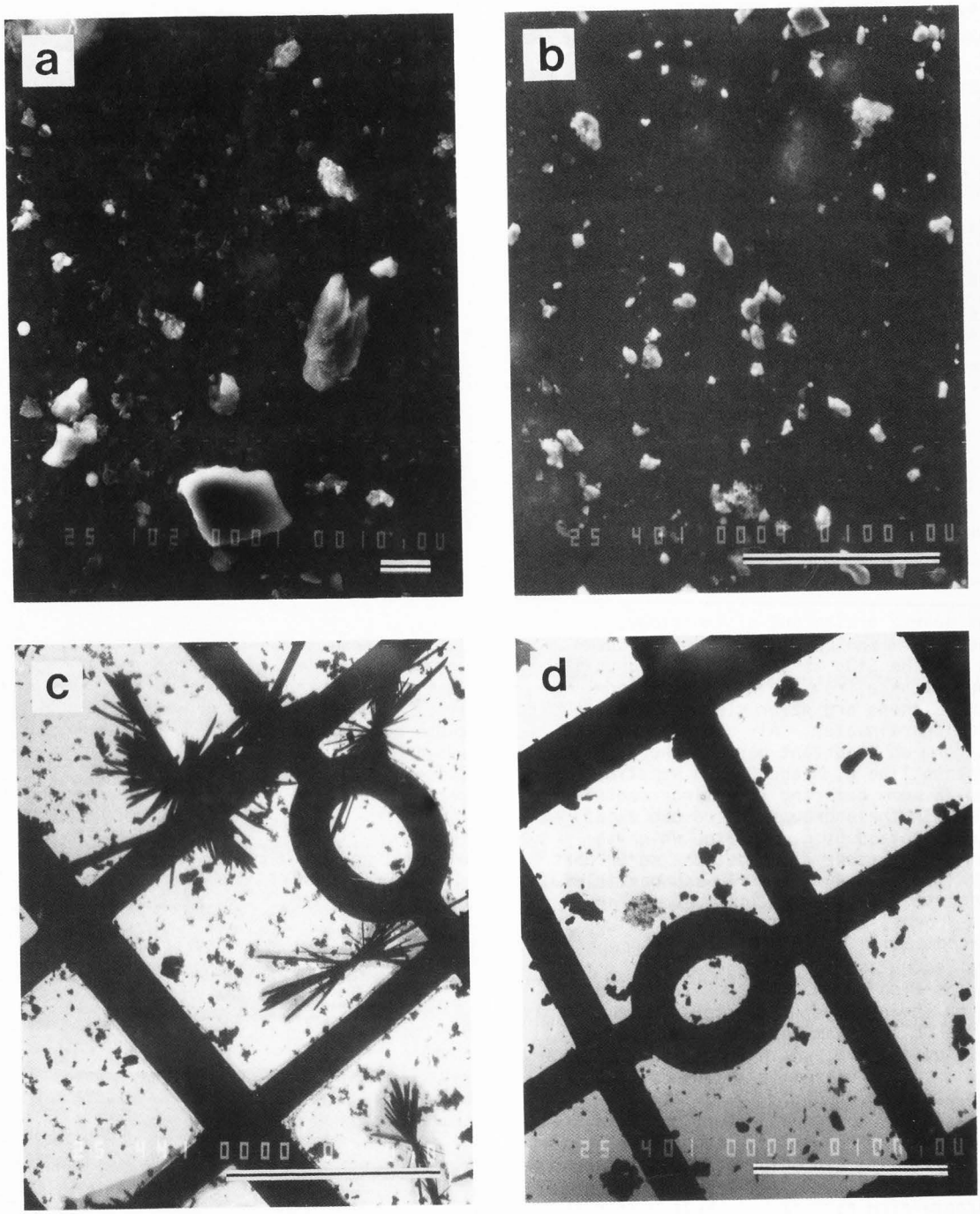

Figure 1 : Typical SEM-micrographs of EPXMA-analyzed suspension particles present in sample B-1 (a) and W-2 (b), and of LAMMA-analyzed bulk and suspension particles, present in B-1 (c) and W-2 (d), and lying on a Formvar coated EM-grid. Bars: (a) 10 μm; (b)-(d) 100 μm.

typical SEM-micrographs of EPXMA analyzed suspension particles present in sample B-1 (a) and W-2 (b). A few typical particles are presented more in detail in Fig. 2.

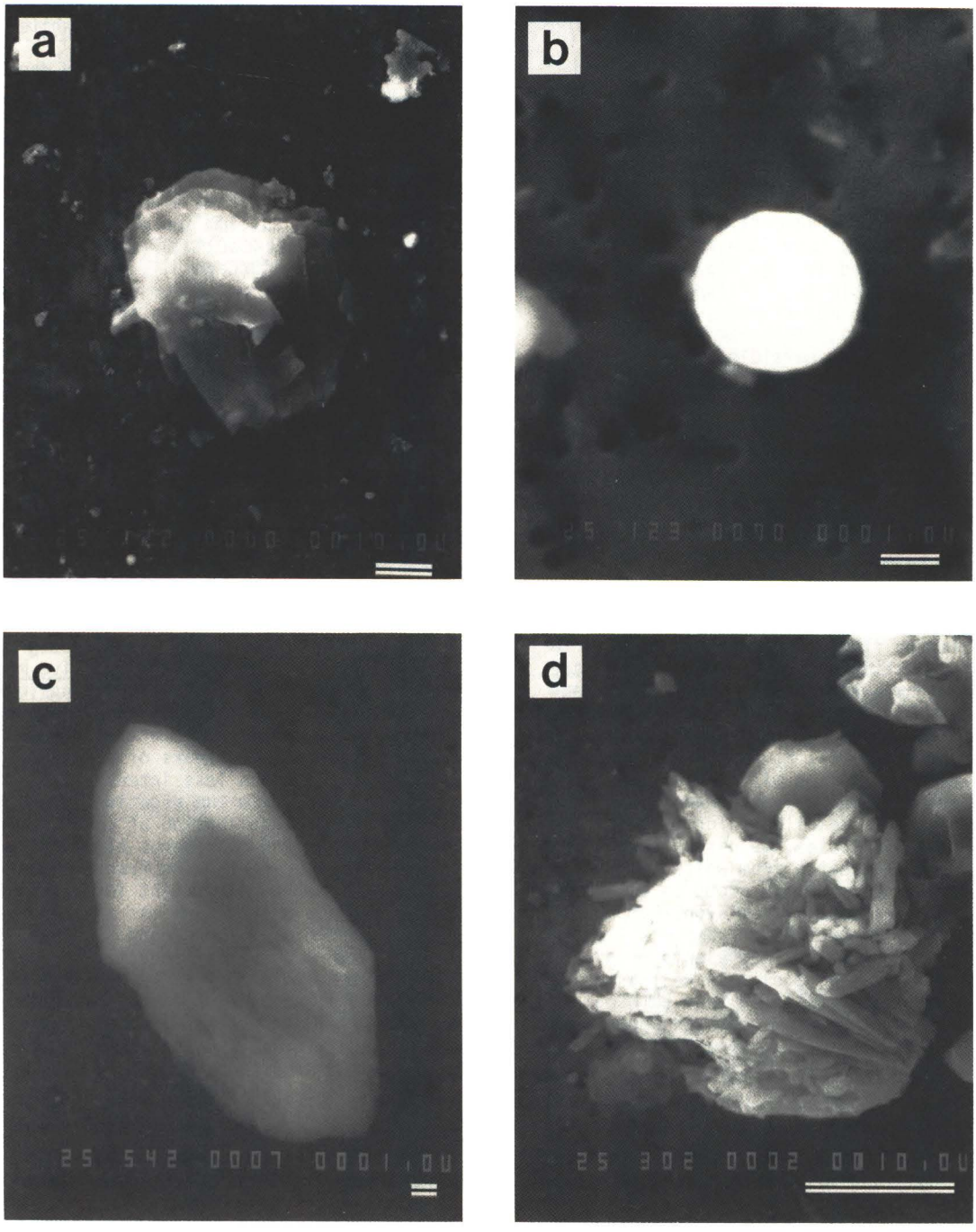

Figure 2 : Characteristic SEM-micrographs of two different fly-ash particle types detected in sample B-1 (a,b) and of original (c) and recrystallized (d) calcite particles present in sample (W-2). Bars: (a), (d) 10 µm; (b), (c) 1 µm.

Results for leachates from black wall section (B-1). In view of the elemental composition of fly-ash particles, according to the publications of Del Monte et al. [3], and of Mamane et al. [13], it is very likely that the Si-, Ca- and Fe-rich groups include some contribution of fly-ash particles. Visual inspection of sample B-1 demonstrated different types of particles that are most likely fly-ash particles. Typical smooth spherically shaped particles, as shown in Fig. 2(b), with a characteristic aluminosilicate matrix are very frequently found. Another characteristic fluffy type with aluminosilicate matrix is represented in Fig. 2(a). Sample group number 10 (Table 1), corresponds to small glassy spheres, with appearance just like the particle of Fig. 2(b). This can be some type of fly-ash though iron-particles from the scaffold will also be present in this sample group. On the contrary, sample group 11 contains fluffy structures. From the backscattered electron image, it can be seen that some particles are heterogeneous; the different elements present are unevenly distributed throughout the particle volume; visual inspection of the particles, showed that the iron was concentrated in some parts of the particle. Sample group number 5 contains differently looking particles, with variable size, shape and morphology. Small spherical particles are present, but also very small and larger fluffy particles contribute to this group. Particles in the organic group are characterized by a high background. By increasing the data acquisition time, one can obtain an idea of the mineral components that are also present (e.g. Al, Si, S, K, Ca and Fe). Carbonaceous fly-ash particles will certainly contribute to this sample group. LAMMA-analysis however, provides more detailed information on the nature of these particles, as discussed below.

Results for leachates from white wall section (W-2). The dominant Ca-rich group in all white samples originates mostly from stone-component erosion. Visual inspection of sample W-2 showed that sample group number 1 represents original calcite-particles (Fig. 2(c)), as well as particles that are recrystallized from $Ca(HCO_3)_2$, being more porous and less smooth in appearance (Fig. 2(d)). In sample W-2, none of the typical spherical aluminosilicate particles (fly-ash) were found.

Laser microprobe study

In order to obtain additional information on the characterization of particulate matter present in the bulk and suspension of the previously described "black" and "white" samples, LAMMA-analysis was performed. With this technique, it is also possible to examine the presence and composition of organic particles. Because of the fact that the recorded mass spectra of the different analyzed sample series were very much alike, from each of them, one typical example namely B-1 and W-2 was selected for discussion.

Fig. 1(c) and (d) show a general view of the particles, present in the bulk and suspension of sample B-1 and W-2 respectively. At first sight, the black sample contains two important particle categories, namely bar-shaped crystals on the one hand, and a group of largely differentiating particles with various shapes, sizes and morphologies on the other hand. In the "white" sample however, no rods could be detected.

Four characteristic positive and negative laser mass spectra of the bar-shaped crystals, detected in the B-1 sample are shown in Fig. 3 (a-d) and (m-p) respectively. The intensities of the major elemental and cluster ion peaks detected in the positive and negative spectra are summarized in Tables 4 and 5, respectively. Besides intense calcium ion peaks, measured at m/e = 40$(Ca)^+$, 56 $(CaO)^+$, 57$(CaOH)^+$, 96 $(Ca_2O)^+$, 112$(Ca_2O_2)^+$ and 113$(Ca_2O_2H)^+$, a high contribution of sodium and potassium elemental ions can be seen in the positive mass spectra. In the negative ion detection mode, besides an intense (S)-ion peak at m/e = 32, a dominant sulphur-oxygen cluster ion pattern at m/e = 48 $(SO)^-$, 64 $(SO_2)^-$ and 80 $(SO_3)^-$ can be detected. From these optical and mass spectral observations, it can be concluded that the bar-shaped crystals mostly consist of gypsum. In general, it has also to be noted that practically no intense aluminum, iron and silicon containing ion peaks were observed in these particles.

After analyzing the other particle category, observed in the B-1 sample, two different groups X and Y can be distinguished. Absolute intensities of selected characteristic spectra are summarized in Tables 4 and 5. A first group X, with two typical positive and negative mass spectra presented in Fig. 4 (e-f) and (q-r) respectively, shows the following spectral behaviour. In the positive detection mode, very intense elemental ion peaks of $(Na)^+$, $(Al)^+$, $(K)^+$ and $(Fe)^+$ and a less intense $(Ca)^+$ peak can be observed. In the negative spectra, besides a high contribution of chlorine, aluminum, silicon and phosphorus cluster ion peaks, a typical carbon-containing fragment pattern has to be remarked. It might indicate that this particle group mostly consists of carbon-rich fly-ash particles. The second, less abundant, group Y with two typical positive and negative mass spectra shown in Fig. 4 (g-h) and (s-t) respectively, gives rise to the detection of intense calcium-containing ion peaks with a minor contribution of chlorine, phosphorus and carbon-containing ions.

Fig. 5 (i-l) and (u-z) show 4 typical positive and negative mass spectra of different particles measured in the W-2 sample. The absolute intensities of major detected ion peaks are summarized in Table 4 and 5. Besides the detection of intense calcium elemental and cluster ion peaks in the positive spectra, in the negative detection mode, an important contribution of silicate and phosphate ion peaks can be remarked. The calcium ions probably originate from recrystallized and original calcium carbonate particles which are leached out of the stone by the overrunning water. Silicate ions in the negative detection mode, and simultaneously measured calcium ions in the positive spectra may indicate calcium silicate structures which also come from erosion of structural limestone components. The presence of phosphorus-contain-

Table 4 : Absolute intensities of elemental and cluster positive ion peaks for different particle groups detected in the "black-1" and "white-2" sample.

Positive ions		Sample B-1								Sample W-2			
m/e	assignment	Bar-shaped crystals				Group X		Group Y		Different particles			
		A	B	C	D	E	F	G	H	I	J	K	L
23	Na	1439	2893	2793	1931	2676	3793	61	272	2839	2136	2500	1188
24	Mg	149	1314	311	181	835	1704	n.d.*	n.d.	951	331	756	320
27	Al	n.d.	123	135	n.d.	2087	3797	n.d.	n.d.	990	88	56	n.d.
28	Si	n.d.	n.d.	n.d.	n.d.	634	906	n.d.	n.d.	n.d.	376	n.d.	n.d.
39	K	2984	4324	3377	2961	3817	4448	994	n.d.	3485	3019	2148	1570
40	Ca	3064	2492	1535	2290	856	864	2381	4279	4137	4524	941	2476
48	Ti	n.d.	162	n.d.	n.d.	317	212	117	321	544	493	362	n.d.
54	Fe	n.d.	n.d.	n.d.	n.d.	334	235	n.d.	n.d.	n.d.	n.d.	n.d.	121
55	Mn	n.d.	n.d.	137	n.d.	n.d.	n.d.	n.d.	n.d.	130	240	n.d.	n.d.
56	CaO; Fe	1470	1321	487	726	2201	1929	1470	2091	3450	3480	1701	898
57	CaOH	1678	1986	1960	2255	232	191	41	1542	2613	2984	1369	1383
59	Co	181	183	n.d.	n.d.	n.d.	n.d.	146	508	1111	952	59	202
63	Cu: Na_2OH	175	338	748	582	346	538	n.d.	n.d.	343	131	319	996
64	Zn	n.d.	n.d.	n.d.	n.d.	121	n.d.	n.d.	n.d.	297	709	n.d.	98
96	Ca_2O	1170	1471	256	264	n.d.	n.d.	1202	1311	1798	3668	2093	1545
112	Ca_2O_2	317	336	155	124	n.d.	n.d	388	475	3487	2989	790	374
113	Ca_2O_2H	608	1266	725	774	n.d.	n.d	62	548	1995	1937	866	200

* n.d. = not detected

Table 5 : Absolute intensities of elemental and cluster negative ion peaks for different particle groups detected in the "black-1" and "white-2" sample.

		Sample B-1								Sample W-2			
Negative ions		bar-shaped crystals				group X		group Y		Different particles			
m/e	assignment	M	N	O	P	Q	R	S	T	U	V	W	Z
32	S	1495	1516	621	1627	148	196	n.d.*	n.d.	n.d.	49	28	295
33	SH	272	483	152	242	135	n.d.	n.d.	n.d.	n.d.	n.d.	136	n.d.
35	Cl	164	791	1411	625	2928	1857	1341	1692	1584	1148	1830	1556
36	C_3	n.d.	146	261	n.d.	894	487	220	1222	49	85	120	326
42	CNO	n.d.	196	445	n.d.	1755	1635	677	419	987	1606	1270	2260
43	AlO	n.d.	n.d.	442	n.d.	1465	1089	367	222	349	662	496	740
46	NO_2	n.d.	n.d.	339	n.d.	635	195	232	66	335	106	n.d.	71
48	SO; C_4	977	1329	915	632	1550	783	322	818	n.d.	573	n.d.	412
59	AlO_2	n.d.	n.d.	509	n.d.	1186	602	295	154	209	507	178	115
60	SiO_2; C_5	n.d.	235	128	n.d.	1953	1354	621	301	1035	1589	1297	1164
62	NO_3; (SiO_2)	n.d.	n.d.	n.d.	n.d.	339	165	48	22	77	99	80	133
63	PO_2	n.d.	n.d.	n.d.	n.d.	2166	3340	780	2076	1736	1332	424	2011
64	SO_2	1713	1490	805	353	344	189	85	101	174	244	n.d.	788
72	C_6	n.d.	n.d.	n.d.	n.d.	978	379	223	327	n.d.	541	n.d.	n.d.
76	SiO_3	n.d.	n.d.	n.d.	n.d.	1360	816	425	97	1068	1724	1204	1693
77	$HSiO_3$	n.d.	n.d.	n.d.	n.d.	1651	797	277	128	325	1022	694	1318
79	PO_3;($HSiO_3$)	n.d.	n.d.	n.d.	n.d.	2716	3088	891	2830	1594	1868	409	2952
80	SO_3	342	42	74	48	80	111	28	73	202	155	120	735
84	C_7	n.d.	n.d.	n.d.	n.d.	408	n.d.	210	301	174	232	n.d.	158
88	FeO_2:Si_2O_2	n.d.	n.d.	n.d.	n.d.	311	320	132	487	129	357	n.d.	92
96	SO_4:C_8	n.d.	n.d.	n.d.	n.d.	479	n.d.	202	33	308	355	n.d.	465
97	HSO_4:H_2PO_4	n.d.	n.d.	n.d.	n.d.	392	n.d.	291	100	n.d.	511	63	434
103	$AlSiO_3$	n.d.	n.d.	n.d.	n.d.	339	n.d.	105	n.d.	n.d.	165	n.d.	275
108	C_9	n.d.	n.d.	n.d.	n.d.	309	n.d.	129	n.d.	n.d.	212	n.d.	201
119	$AlSiO_4$	n.d.	n.d.	n.d.	n.d.	899	152	209	n.d.	n.d.	n.d.	382	n.d.
120	C_{10}	n.d.	n.d.	n.d.	n.d.	121	n.d.	110	n.d.	n.d.	n.d.	378	n.d.
133		n.d.	n.d.	n.d.	n.d.	212	n.d.	152	n.d.	n.d.	n.d.	232	n.d.

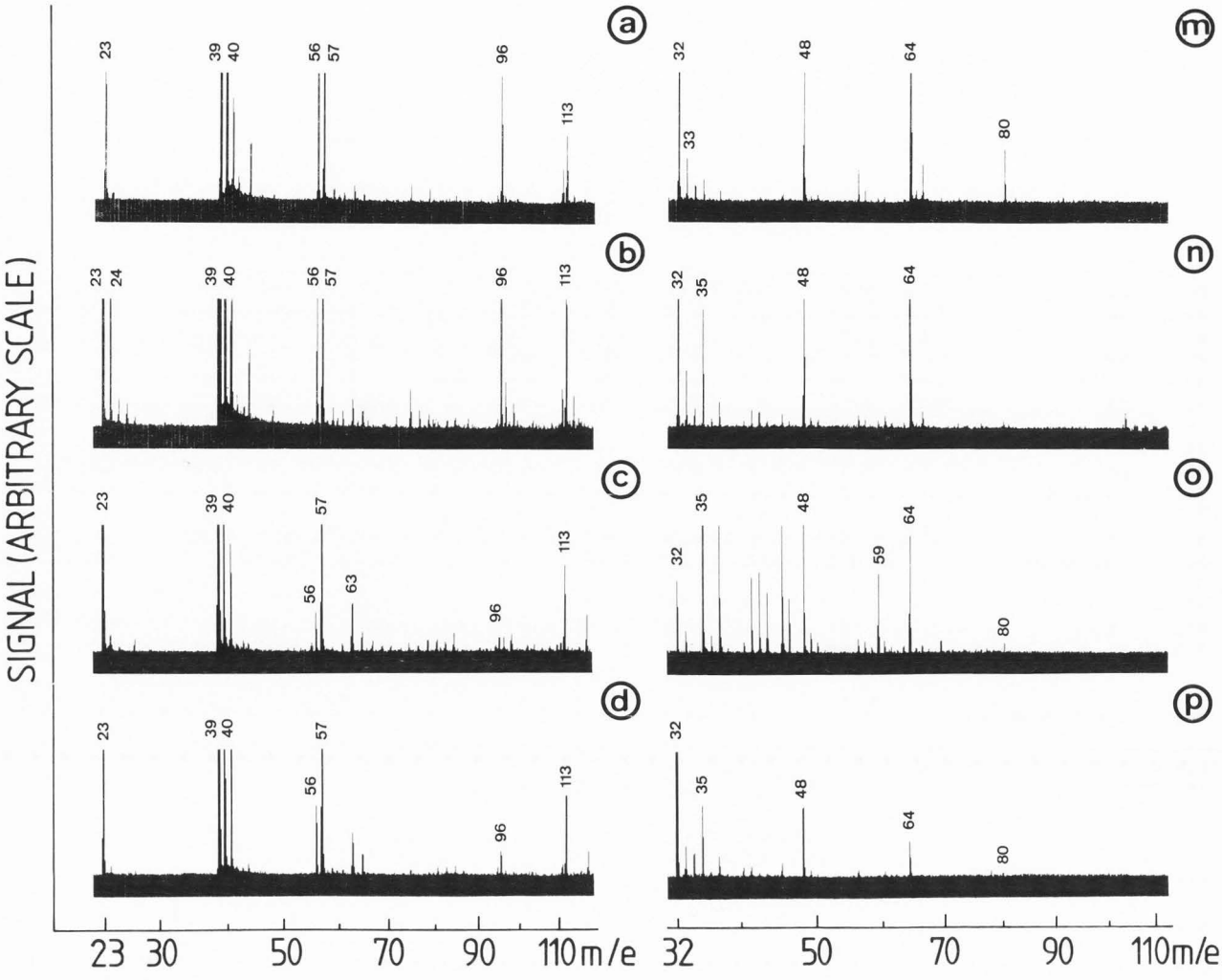

Figure 3 : Characteristic positive (a-d) and negative (m-p) mass spectra of bar-shaped crystals present in the bulk and suspension of sample B-1.

ing ions may indicate the contamination of the stone sample by bird droppings.

Conclusions

Automated EPXMA revealed an important difference in the composition of suspended particles, present in leaching water from black and white wall sections. The suspension of black wall's run-off is characterized by a dominant Si-rich group, originating mostly from impaction of airborne particulate matter, while white walls give rise to a major Ca-rich group in their leaching water. Visual inspection showed that the important silicon-rich group in the "black" samples is mostly composed of fly-ash particles. Furthermore, different types of fly-ash were observed in the "black" samples. The predominant Ca-rich group in the "white" samples, contains both original and recrystallized calcite particles.

LAMMA-analysis could further provide valuable information on the characteristics of particles, present in suspension and in the bulk. Gypsum-rods could be detected in "black", but not in "white" samples, this fact is in good agreement with the bulk analysis results and with the EPXMA-study. LAMMA also showed that the particles, characterized by EPXMA as 'organic', are composed of carbon. In general, LAMMA showed gypsum rods, Na-Al-K-Fe-C-rich particles, and a very small group Ca-rich particles in the "black" samples, and predominantly Ca-rich and Ca-Si particles in the "white" samples.

It can be concluded that black wall sections are entirely covered with a gypsum crust, that turns black, due to adhesion of soil dust and common air pollutants, especially fly-ash. Black crusts are mostly seen at sites protected from direct rainfall but their occurrence depends also significantly on the individual stone characteristics. White wall sections, which have fresher

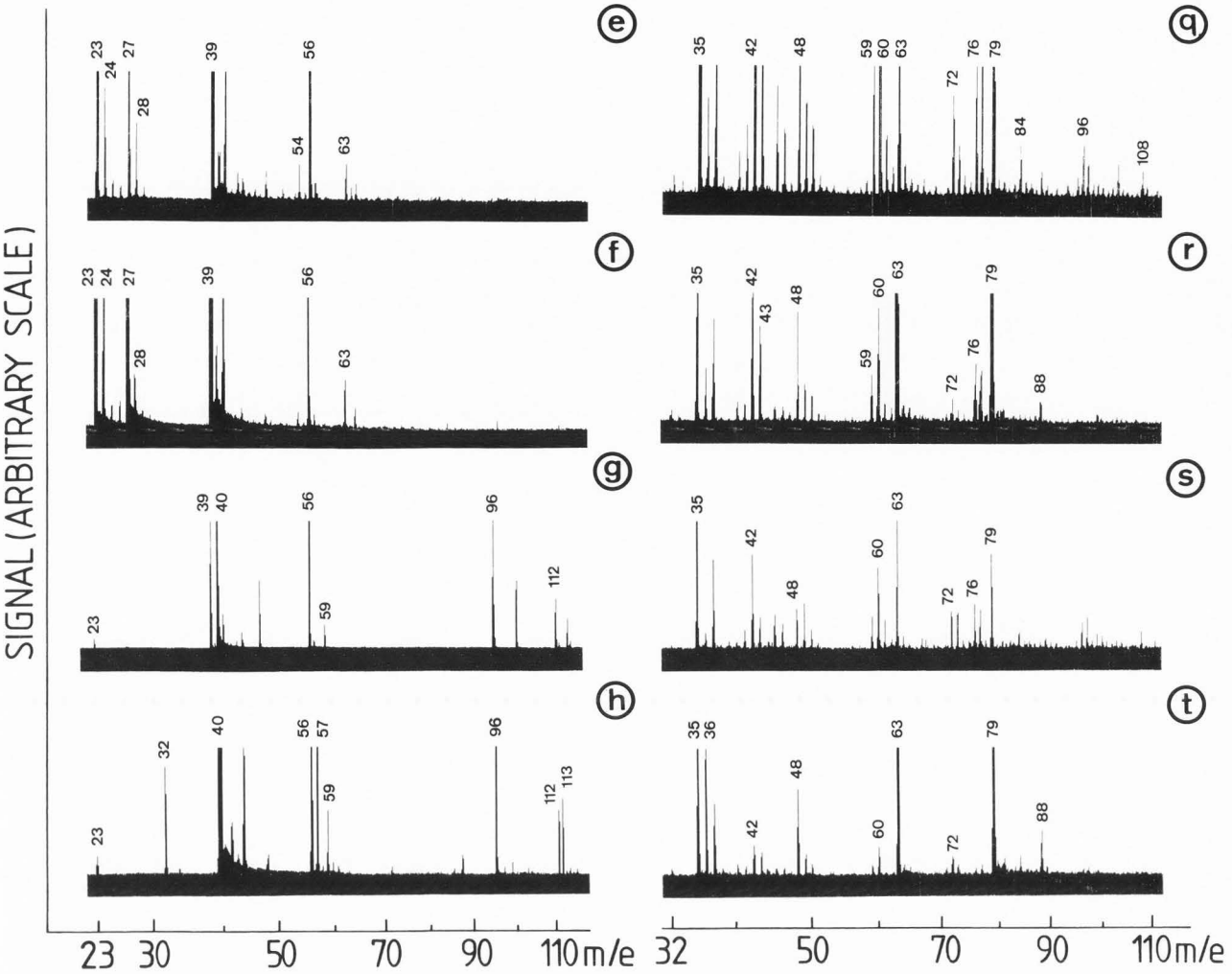

Figure 4 : Typical positive (e-h) and negative (q-t) mass spectra of group X (e,f,q,r) and group Y (g,h,s,t) particles present in the bulk and suspension of sample B-1.

appearance, because the weathering products are carried away by the overrunning rainwater, undergo accelerated erosion.

Acknowledgements

This study was partially financed by the Commission of the European Communities under contract no. EV3V-0928-B (GDF). One of us (JKDW) is indebted to the National Fund for Scientific Research (NFWO, Belgium), for financial support.

References

1. Bernard P, Van Grieken R, Eisma D (1986) Classification of estuarine particles by automated electron microprobe analysis and multivariate cluster techniques. Envir. Sci. Technol. 20, 467-473.

2. Camuffo D, Del Monte M, Sabbioni C, Vittori O (1982) Wetting, deterioration and visual features of stone surfaces in an urban area. Atmosph. Envir. 16(9), 2253-2259.

3. Del Monte M, Sabbioni C, Vittori O (1981) Airborne carbon particles and marble deterioration. Atmosph. Envir. 15(5), 645-652.

4. Del Monte M, Sabbioni C, Vittori O (1984) Urban stone sulphation and oil-fired carbonaceous particles. Sci. Tot. Envir. 36, 369-376.

5. Denoyer E, Van Grieken R, Adams F, Natusch D (1982) Laser microprobe mass spectrometry 1 : basic principles and performance characteristics. Anal. Chem. 54, 26A-41A.

6. Graedel TE, Mc Gill R (1986) Degradation of materials in the atmosphere. Env. Sci.Technol. 20(11), 1093-1100.

7. Hercules DM, Day RJ, Balasanmugam K, Dang TA, Li CP (1982) Laser microprobe mass spectrometry 2 : applications to structural analysis. Anal. Chem. 54, 280A-305A.

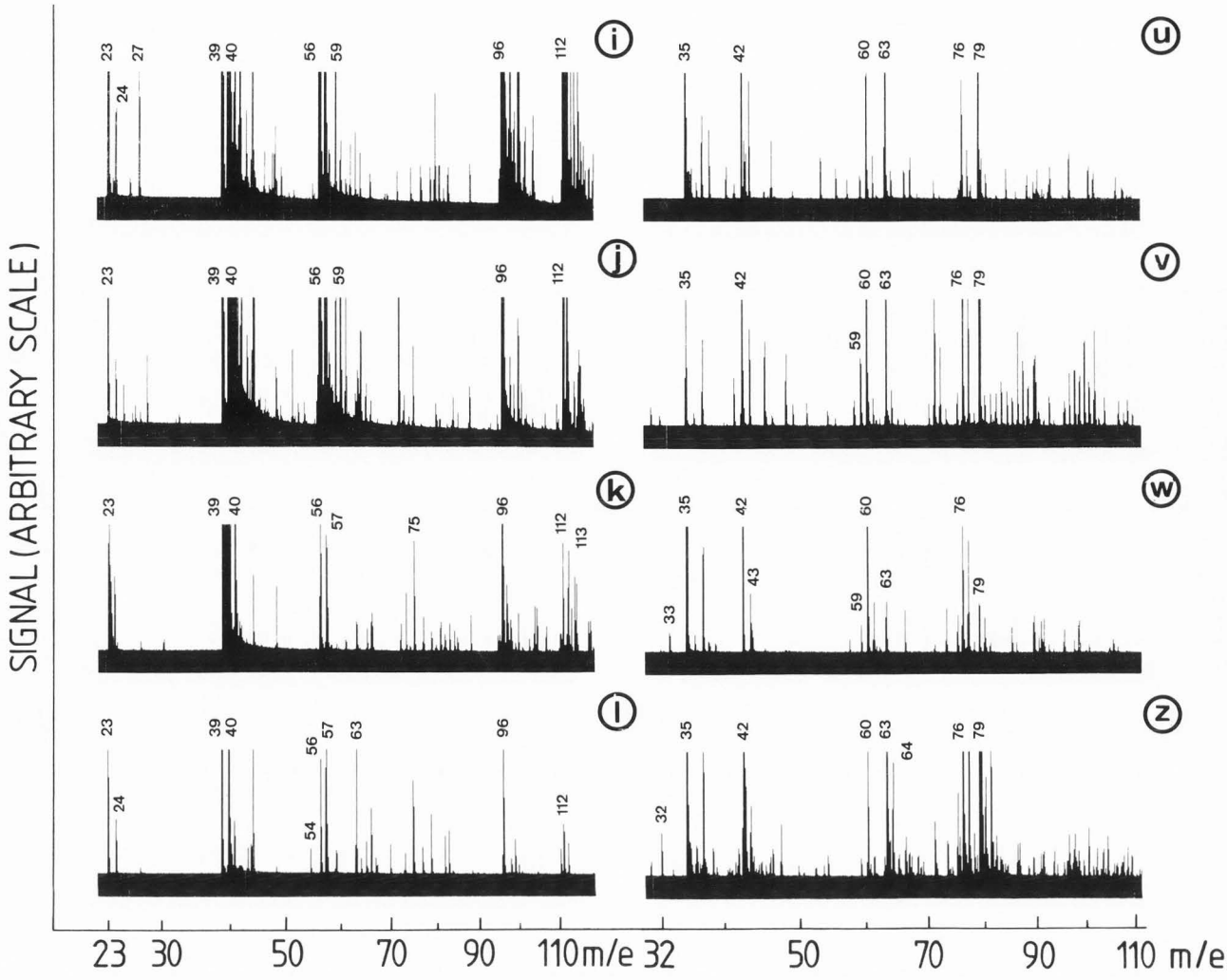

Figure 5 : Characteristic positive (i-l) and negative (u-z) mass spectra of particles, present in the bulk and suspension of sample W-2.

8. Kaufmann R, Hillenkamp H, Wechsung R (1979) The laser microprobe mass analyzer (LAMMA) : a new instrument for biomedical microprobe analysis. Med. Prog. Technol. 6, 109-121.

9. Keppens E, Roekens E, Van Grieken R (1985) Effect of pollution on sandy limestones of a historical cathedral in Belgium. Proc. 5th Int. Congress on Deterioration and Conservation of Stone, Lausanne, 25-27 September , Presses Polytechnique Romandes Vol. 1, p. 499-507.

10. Leysen L, Roekens E, Storms H, Van Grieken R (1987) Classification of suspended particles in deposition samples and run-off water samples from a limestone cathedral. Atmosph. Envir., in press.

11. Leysen L, Roekens E, Komy Z, Van Grieken R (1987) Micro- and trace analysis study of the weathering of a historical building. Anal. Chim. Acta, in press.

12. Livingston RA (1986) Evaluation of building deterioration by water run-off. Building Performance : function, preservation and rehabilitation. ASTM STP 901. G. Davis, Ed., American Society for Testing and Materials, Philadelphia, 181-188.

13. Mamane Y , Miller J, Dzubay T (1986) Characterization of individual fly-ash particles emitted from coal- and oil-fired power plants. Atmosph. Envir. 20(11), 2125-2135.

14. Massart D, Kaufman L (1983) The interpretation of analytical chemical data by the use of cluster analysis, Chemical Analysis Series no. 65, John Wiley, New York, 237 pp.

15. Nijs R (1985) Petrographical characterization of calcareous building stones in Northern Belgium.Proc. 5th Int. Congress on Deterioration and Conservation of Stone, Lausanne, 25-27 September,Presses Polytechnique Romandes Vol. 1, p. 13-21.

16. Proceedings of the 2nd International Colloquium on Materials Science and Restoration (1986) Esslingen, 2-4 September , F.H. Wittmann, Ed. 736 pp.

17. Raeymaekers B (1986) Characterization of particles by automated electron probe micro-

analysis. Ph.D. Thesis, University of Antwerp (UIA), Antwerp-Wilrijk, Belgium.

18. Roekens E , Leysen L , Komy Z , Van Grieken R (1986) Chemical characterization of weathering crust and run-off water for a deteriorated limestone cathedral. Proc.2nd Int.Colloq. on Materials Science and Restoration, Esslingen, 2-4 September 1986, F.H. Wittmann,Ed.487-489.

19. Roekens E, Van Raemdonck C, Leysen L, Chakravorty R, Van Grieken R (1987) Weathering products and surface recession rates for sandy limestones exposed to air pollution. Proc. Int. Conference on Acid Rain, Lisbon 1-3 September, in press (copy available from authors).

20. Van Espen P (1984) A program for the processing of analytical data (DPP). Anal. Chim. Acta 165, 31-49.

21. Van Espen P, Van Vaeck L, Adams F (1986) Transient recorders : a key-element in the laser microprobe mass spectrometry. Proc. 3th Int. Laser Microprobe Mass Spectrometry Workshop Antwerp 26-27 August, University of Antwerp p. 195-198.

22. Van Gemert D, Vanden Bosch M, Van Eyck-Debrouwer D, Van Meer H (1986) Evaluation of accelerated corrosion tests for natural stone. Proc. 2nd Int. Colloquium on Materials Science and Restoration, Esslingen 2-4 September, p. 497-503.

23. Vogt H, Heinen J, Meier S, Wechsung R (1981) LAMMA 500 principle and technical description of the instrument.Fresenius'Z. Anal. Chem. 308, 195-200.

Discussion with reviewers

R.A. Livingston : Can similar particle analyses be made in the rainwater run-off samples?
Authors : Indeed, this can be done and we have applied it to deposition and run-off samples, collected at the same cathedral. The results were reported in ref. 10 (Classification of suspended particles in deposition samples and run-off water samples from a limestone cathedral, Atmosph. Environ., in press). It was found that run-off samples were enriched largely in Ca-containing suspension particles, in comparison to deposition samples, where the Si-rich group was the most abundant one. This confirms that the rainwater, which has a high pH at the site of the cathedral due to the washout of atmospheric $CaCO_3$ particles originating from the wind erosion of the building or from the emission of the restoration work place, plays an important role as an eroding medium. Different stone components, especially $CaCO_3$, but also quartz particles, are leached out by the overrunning rainwater. Furthermore, considering the large SO_4^{2-} concentration in solution and the small amount of undissolved $CaSO_4$ particles that were found in the run-off water, it was concluded that the deterioration product gypsum is mostly removed by dissolution in the run-off water, or eroded away as particles, which dissolve afterwards in the collection vessel.

R.A. Livingston : To understand the significance of the clusters presented in Tables 1 and 2, would it not be helpful to include dendograms?
Authors : We do not believe that presenting a dendogram would be helpful or even feasible : the drawing would have, for a typical analysis of 400 particles in one sample, some 400 vertical lines at the bottom.

R.A. Livingston : It would be interesting to have mass balance calculations giving the rate of erosion from the black and from the white areas, and the relative contributions of particles and solutes to the total rate.
Authors : These calculations are presented in detail in ref. 19 (Weathering products and surface recession rates of sandy limestones exposed to air pollution, Proc. Int. Conference on Acid Rain, Lisbon 1-3 September, in press). The mean yearly material losses, weighted to the volume of rainfall, are 20 g $CaCO_3/m^2$ (solute) and 27 g particulate/m^2 respectively. The mean yearly surface recession was found to be around 20 µm.

Reviewer III : So much work has been published on gypsum crusts and their formation that the authors do not seem to be adding anything new, other than the application of a newer technique to a previously understood problem. I feel that the authors should give more justification as to why they felt it necessary to re-analyse a well understood problem.
Authors : We studied a building constructed with sandy limestones of Balegem and Gobertingen, which are typical Belgian stones, used in many old important historical buildings. For these specific stone types, to our knowledge no work has ever been published on their air pollution induced deterioration mechanism. Since these types of stones are very sensitive to air pollution-induced decay, a detailed and thorough examination of the deterioration mechanism and evaluation of the possible presence of catalyzing particles in the weathering crust is justified and necessary to give enough scientific basis to the government policy of restoration and protection of weathered historical buildings. Moreover, for the air pollution situation in Flanders (and Western Europe), the relative importance in building deterioration of SO_2 and NO_x has never been documented, although it is of prime importance for the abatement strategy. Furthermore, recent publications point to the important role of soot and fly-ash particles as catalyzing agents in the weathering process; micro-analytical techniques such as EXPMA and LAMMA are well suited to gain information on these types of particles.
Reviewer IV : Why are the authors studying leachings rather than the samples from the walls themselves?
Authors : A detailed study was performed to elucidate the general chemical deterioration mechanism of St. Rombout's Cathedral of which the integral results are described in a review paper, entitled "Air pollution induced chemical decay of a sandy limestone cathedral in Belgium", submitted to Science of the Total Environment. In this study, thin sections of stones and slates, pieces of surface weathering crust and underlying crust layer, total, wet and dry deposition

samples, samples of rainwater run-off, and leaching water, were all thoroughly examined. This paper reports only the results of the latest experiment, the production of artificial run-off water, or leaching water.
The leaching technique was evaluated versus the run-off water. It is not rain dependent, requires no attachment of collectors to the building and allows the isolation of specific wall sections in order to study these separately.

Reviewer IV : The pH of rainwater and total deposition, collected near the cathedral was slightly alkaline, compared to normal pH-values of pure rainwater. What is meant by slightly alkaline? Is it this alkalinity that the authors use to conclude that it is gaseous SO_2 that is the offending agent?
Authors : The pH value of total deposition is on the average around 6.7, and that of rainwater is 5.8, while the natural pH of rainwater is 5.6. The conclusion that SO_2 is the offending agent is mostly based on the fact that the pH of local rainwater is near the natural value, and on the observation that also at places which are not wetted by rain, a thick gypsum crust is found on the stones.

Reviewer IV : Are the actual conditions of the substrates better or worse on the black or the white walls? Is it a good idea to remove the black crust? In many cases the black crusts are a sign of a very badly deteriorated substrate. It appears that this is not the case here. Is this in any way stone-related or is it simply prevailing wind-related?
Authors : Black crusts are indeed often a sign of a seriously deteriorated substrate. Their occurrence is surely related to the prevailing wind direction, but moreover individual stone characteristics are extremely important : very deteriorated stones were found next to much less deteriorated stones, although both were exposed to similar atmospheric conditions. White stone walls have often a cleaner appearance which is however caused by the continuous removal of reaction products by the rainwater, so that the decay is faster than on black stone sections.

M. Montoto : Could your method be applied to interpret the presence or absence of soil patina not related to atmospheric agents, for instance to a possible static electrical charge on the rock surface.
Authors : With the applied techniques, it is possible to give an exact description of particles that are found at the surface of materials, e.g. stones. By careful consideration of the local pollution situation and the different particle types that are found in deposition samples and air samples, collected at the site of the cathedral, we can make estimations about the possible sources of particles, found at the surface of the stones i.e. whether they originate from the stone itself (e.g. $CaCO_3$ particles, SiO_2-particles), whether they are pollution induced (e.g. S-containing carbonaceous fly-ash particles) or result from the scaffold (e.g. Fe-oxides). Whether particles are found, due to a static electrical charge on the rock surface, cannot be elucidated with the method that we applied here.